Langmuir

Article

pubs.acs.org/Langmuir

Unraveling Dendrimer Translocation Across Cell Membrane Mimics

Anna Åkesson,[†] Tania K. Lind,[†] Robert Barker,[‡] Arwel Hughes,[§] and Marité Cárdenas*,[†]

[†]Institute of Chemistry and Nano-Science Center, University of Copenhagen, Universitetsparken 5, DK 2100 Copenhagen, Denmark

[‡]Institut Laue Langevin, BP 156, 6 rue Jules Horowitz, 38042 Grenoble Cedex 9, France

[§]Rutherford Appleton Laboratory, Harwell Oxford, Didcot OX11 OQX, United Kingdom

Supporting Information

ABSTRACT: Poly(amidoamine) (PAMAM) dendrimers are promising candidates in several applications within the medical field. However, it is still to date not fully understood whether they are able to passively translocate across lipid bilayers. Recently, we used fluorescence microscopy to show that PAMAM dendrimers induced changes in the permeability of lipid membranes but the dendrimers themselves could not translocate to be released into the vesicle lumen. Because of the lack of resolution, these experiments could not assess whether the dendrimers were able to translocate but remained attached to the membrane. Using quartz crystal microbalance with dissipation monitoring and neutron reflectivity, a structural investigation was performed to determine how dendrimers interact with zwitterionic and negatively charged lipid bilayers. We hereby show that dendrimers adsorb on top of lipid bilayers without significant dendrimer translocation, regardless of the lipid membrane surface charge. Thus, most likely dendrimers are actively transported through cell membranes by protein-mediated endocytosis in agreement with previous cell studies. Finally, the higher activity of PAMAM dendrimers for phosphoglycerol-containing membranes is in line with their high antimicrobial activity against Gram-negative bacteria.

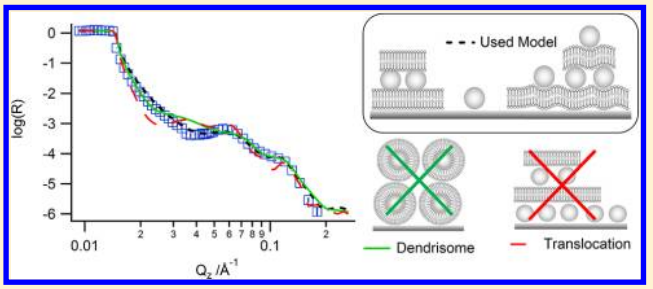

INTRODUCTION

Poly(amidoamine) (PAMAM) dendrimers are unique monodisperse polymers with tunable size and surface properties. They consist of an internal core, layers (generations) of repeating branches, and external terminal groups, which can easily be modified. These unique structural properties turn dendrimers into promising molecules for various applications in the medical field. Pharmaceutical agents can be both covalently and noncovalently attached to the dendrimer, and both protective and targeting motifs can be attached to the terminal groups.[1−5] PAMAM dendrimers were the first group of dendrimers to be fully characterized in the mid-1980s,[6] and they have been extensively investigated since then. However, there have been controversies about the mechanism by which PAMAM dendrimers enter into cells. Dendrimers were proposed to enter the cell through an active process mediated by membrane proteins.[7−10] However, dendrimers have been shown to create holes in lipid bilayers, which might result in passive dendrimer translocation across the cell membrane.[11−16] Using fluorescence microscopy, we have recently shown that, even though dendrimers are able to destabilize the structure of lipid vesicles, they do not appear to translocate across the vesicle membrane to be released into the vesicle lumen.[17] However, fluorescence microscopy lacks the resolution to determine if the dendrimers are intercalated in the lipid membrane or if they are able to translocate but remain attached to the other side of the membrane. Neutron reflectivity (NR) and quartz crystal microbalance with dissipation monitoring (QCM-D) applied to supported lipid bilayers (SLBs) offer a unique combination of techniques to address this issue. QCM-D can sense interfacial processes even at very low surface concentrations (ng/cm^2), while NR is excellent at identifying the structure of interfaces down to a 5 Å resolution, when fitting multiple contrasts simultaneously. In this work, we have investigated the interaction between the PAMAM dendrimer of generation six (G6) with SLBs composed of 1-palmitoyl-2-oleoyl-*sn*-glycero-3-phospho-(1′-*rac*-glycerol) (POPG) and 1-palmitoyl-2-oleoyl-*sn*-glycero-3-phosphocholine (POPC). We were thereby able to probe the effect of PAMAM dendrimers of G6 on SLBs with increasing negative charge, to determine if translocation can be achieved or promoted, by increasing the electrostatic interactions between the lipids and dendrimers.

EXPERIMENTAL SECTION

Materials. Milli-Q purified water was used in all experiments. D_2O was provided from the neutron sources at ILL, Grenoble, France, and ISIS, Didcot, U.K. POPC, 1-palmoyl(d_{31})-2-oleoyl-*sn*-glycero-3-phosphocholine (d_{31}-POPC), and POPG dissolved in chloroform were purchased from Avanti Polar Lipids and used without further purification. Phosphate buffer (Na_2HPO_4 and NaH_2PO_4) and sodium chloride (NaCl) were purchased from Fluka Biochemika and Sigma Aldrich, respectively. PAMAM dendrimers with an ethylenediamine core of generation 6 (PAMAM G6) in methanol were purchased from

Received: July 6, 2012
Revised: August 10, 2012
Published: August 14, 2012

Sigma Aldrich. Before usage, methanol was removed under a stream of N_2 and dendrimers were dissolved in phosphate-buffered saline (PBS) buffer (10 mM sodium phosphate and 100 mM NaCl at pH 7.4).

Vesicle Preparation and SLB Formation. SLBs were created by fusion of sonicated vesicles, as previously described.[18] Shortly, lipid suspensions were mixed in appropriate conditions, and chloroform was evaporated under a stream of N_2 and placed in a vacuum chamber for at least 1 h to create the lipid film. The lipid films were resuspended in Milli-Q to a concentration of 1 mg/mL and incubated at ambient conditions for at least 1 h. Sonication were performed with a tip sonicator, Misonix sonicator 3000 (Misonix, Inc.), until almost clear solution was obtained. Thereafter, the solution was diluted to 0.5 mg/mL, and sonication continued until the solution was completely transparent. Before injection of vesicle solution to the experimental cells, 2 mM $MgCl_2$ was added to the lipid solution containing POPG to make the lipid vesicles attach to the solid support. After injection of lipid solution, the vesicles were allowed to diffuse and adsorb to the surface for 15 min before excess vesicles were rinsed off with first water and then PBS buffer. For NR measurement on POPC bilayers, lipids with one of the tails predeuterated (d_{31}-POPC) were used, while fully hydrated lipids were used in all other experiments.

NR. Specular NR[19] is an excellent technique to measure structure and composition of an adsorbed thin layer in the direction perpendicular to the interface, in a non-destructive way. The specular reflection $R(Q)$, defined as the ratio between the reflected and incoming beam, is measured as a function of the wave-vector function $Q_z = 4\pi \sin\theta/\lambda$, where λ is the wavelength and θ is the angle between the incoming beam and the reflecting surface. The sensitivity of the measurement depends upon the contrast in nuclear scattering length density (SLD) between the sample and surrounding medium. The SLD of a medium is related to the composition density by SLD = $\sum_j n_j b_j$, where n_j is the number of nuclei found in a given volume and b_j is the coherent scattering length. The contrast can be changed by isotopic substitution, where hydrogen is changed to deuterium, giving a large change in scattering but no change in the chemical composition, thus making neutron scattering techniques particularly suited for biological systems. The studies were performed using solid−liquid experimental cells, where the incoming beam passes through the silicon block and becomes reflected at the interface with the aqueous solution. Silicon (Si) surfaces were polished and heated for 10 min in 7:3 H_2SO_4/H_2O_2 at 80 °C before each experiment. The surfaces and liquid flow cells were quickly assembled under continuous water flow to minimize any surface contamination. The reflectometer SURF at ISIS, STFC Rutherford Appleton Laboratory (Didcot, U.K.)[20] was used for measurement on the POPC bilayer, while the reflectometer D17 at Institut Laue Langevin (Grenoble, France)[21] was used for measurement on the mixed POPC/POPG bilayer. In all experiments, the temperature was controlled using a water bath set to 25 °C. Surfaces were precharacterized before injection of vesicles, which were allowed to equilibrate for 30 min before rinsing with water, and the bilayers were characterized using two to three solvent contrasts: water (H_2O), heavy water (D_2O), and 38 vol % D_2O, with the latter giving a water contrast corresponding to SLD_{Si} (cmSi). After SLB characterization, ∼10 mL of dendrimer solution was flushed and left to adsorb for 3 h before NR characterization. Then, the surface was rinsed off with D_2O, H_2O, and cmSi, and NR profiles were measured at each step. Rinsing with excess buffer after dendrimer exposure did not affect the interfacial structure of either SLB, as shown in Figure S6 of the Supporting Information. All NR profiles obtained in this study were fitted by simulation using the Motofit[22] package, which uses the Abeles matrix method to calculate the reflectivity of thin layers. The SLD, thickness (d), solvent penetration (φ), and interfacial roughness between the layers (σ) are the parameters that characterize each layer. The bare surface was fitted to a two-layer model (Si−SiO_2), and the bilayers were fitted to a three-layer model consisting of headgroups−lipid tails−headgroups. The water distribution in all layers was restricted to maintain identical mean molecular areas (MMAs) for the headgroups and the lipid tails to keep a physically realistic bilayer model. Physical properties for the used lipids can be found in Table 1.

Table 1. Physical Properties for the Used Lipids

lipid		SLD ($\times 10^{-6}$, Å^{-2})	volume (Å^3)	reference
d_{31}-POPC	head	1.85	322	23
	tail	3.2	934	
POPC	head	1.85	322	23
	tail	−0.3	934	
POPG	head	2.33	289	24
	tail	−0.3	914	

QCM-D. QCM-D measurements were performed with a Q-SENSE E4 system (Q-Sense, Västra Frölunda, Sweden). The sensor crystals used were coated with 50 nm silicon oxide, purchased from Q-Sense. For cleaning, the sensor surfaces were placed in 2% Hellmanex (Hellma Analytics, Germany) for 10 min, followed by thorough rinsing in absolute ethanol and ultrapure water. The surfaces were dried in a stream of nitrogen and oxidized in an ultraviolet (UV) ozone chamber (BioForce Nanosciences, Inc., Ames, IA) for 10 min to remove all contamination. O-rings were placed in 2% Hellmanex for 10 min, followed by careful rinsing in ultrapure water and drying in a stream of nitrogen. Before measurements, the instrument temperature was equilibrated to 25 °C. The fundamental frequency (5 MHz) and six overtones (3rd, 5th, 7th, 9th, 11th, and 13th) were found and recorded in PBS. The cells were then rinsed with Milli-Q before the lipids (0.5 mg/mL) dissolved in Milli-Q were pumped into the cells at 100 μL/min until a stable signal was obtained. After bilayer formation, the membranes were rinsed with excess H_2O and PBS before the dendrimers were pumped through the system. For the addition of PAMAM dendrimers to POPG-containing membranes, the continuous flow was stopped 6 min after injection of dendrimers to the cell, to resemble the experimental setup for NR measurements.

RESULTS

We investigated the interaction of PAMAM G6 dendrimers with SLB composed of POPC only and POPC/POPG mixtures at a molar ratio of 3:1 at physiological-like conditions in terms of pH and salinity. The human cell membrane consists to a large extent of PC lipids,[25] making POPC bilayers a relevant model system for investigations of nanoparticle interaction with model cell membranes. However, most biological membranes have a net negative charge, thus making it relevant to investigate the effect of negatively charged membranes. For this, we have chosen to add negatively charged POPG lipids, which are one of the major components in *Escherichia coli* cells,[26] to POPC membranes. Thereby our models can be used as simple systems for mammalian and *E. coli* cell membranes.

We first titrated the SLBs with dendrimers using QCM-D. The QCM-D signal is characterized by a change in frequency and dissipation, both related to the properties of the adsorbed film. Adsorption of mass to the crystal surface gives rise to a frequency decrease, while the viscoelastic properties of the adsorbed film are assessed via the dissipation change. If the adsorbed layer is soft/viscous, it will not follow the crystal oscillations perfectly, causing an internal friction because of film deformation, hence increased dissipation. Using QCM-D, we identified relevant conditions to maximize the dendrimer−lipid interaction, and then NR was performed to obtain maximum structural information.

POPC Bilayers. Figure 1 gives QCM-D data for the titration of PAMAM G6 to POPC SLBs with concentrations ranging from 0.1 to 8 μM. For clarity, only the 7th harmonics are shown, and the graphs are offset to zero after bilayer formation just prior to dendrimer injection (for a typical bilayer formation signal, see Figure S1 of the Supporting Information, and for data containing several harmonics, see Figure S2 of the

dx.doi.org/10.1021/la3027144 | *Langmuir* 2012, 28, 13025−13033

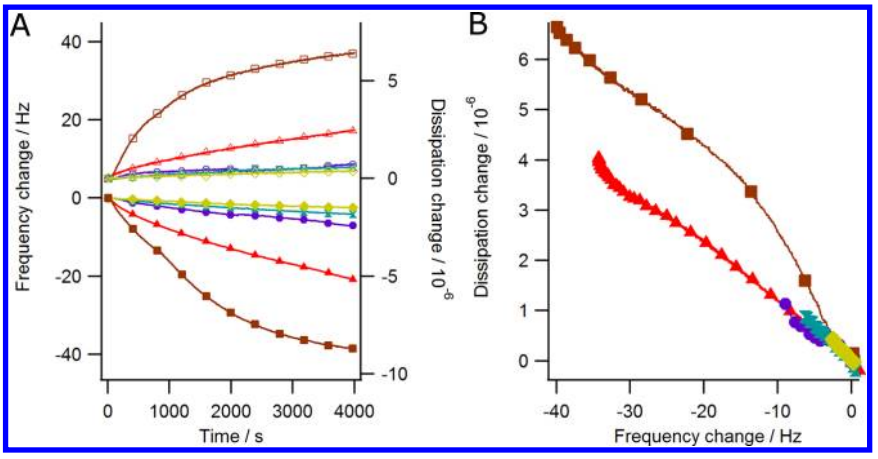

Figure 1. Dendrimer adsorption on SLBs composed of pure POPC. Measurements for the addition of five dendrimer concentrations, 0.1 μM (rhomb, green), 0.5 μM (double-triangle, blue), 1 μM (circle, purple), 5 μM (triangle, red), and 8 μM (square, brown), are shown. (A) Change in frequency (filled symbols) and dissipation (open symbols) upon dendrimer addition. (B) Change in dissipation against change in frequency after dendrimer addition to a POPC bilayer. For clarity, an offset is performed prior to dendrimer addition, only the 7th harmonics are shown, and only 10% of the measured points are shown as markers. Typical frequency and dissipation changes for SLB formation are shown in Figure S1 of the Supporting Information, while several overtones are given in Figure S2 of the Supporting Information.

Supporting Information). At time t = 0 s, the SLB is exposed to dendrimers, leading to a decrease in frequency, typically associated with adsorption of mass. At the same time, an increase in dissipation is observed. This behavior is associated with increased viscosity of the adsorbed layer, as expected. The dendrimer interaction with the POPC bilayer is concentration-dependent and appears to be related to a pure adsorption mechanism, as demonstrated in the dissipation/frequency (D/F) plot shown in Figure 1B, where a linear dependence is observed for all concentrations. For the highest dendrimer concentration used, 8 μM, a second linear regime with less steep slope is observed, indicating that the dissipation increase (upon frequency decrease) is larger at low coverage. This could be due to enhanced movement of trapped liquid and dendrimers on top of the bilayer at low dendrimer surface coverage, as previously observed for adsorption of heterogeneous films.[27−29] Interestingly, constant dendrimer adsorption occurs only upon continuous flow, while steady state is quickly reached once the flow is stopped (Figure 2), thus indicating the importance of the mass-transfer conditions at the interface upon measurement.

Neutron reflection measurements on a perdeuterated POPC (d_{31}-POPC) SLB before and after the addition of 8 μM PAMAM G6 dendrimer are shown in Figure 3 for three isotopic contrasts: water (H_2O), heavy water (D_2O), and water contrast matched to silicon (cmSi). A nearly perfect SLB was formed, having a surface coverage of 4.0 ± 0.6 mg/m^2. This value can be compared to the theoretical maximum of 3.9 ± 0.2 mg/m^2 for a POPC bilayer in the fluid phase.[30] Almost no change is observed upon the addition of 8 μM PAMAM G6 dendrimer. However, the data can be fitted to adsorption of 1% dendrimer on top of an intact bilayer. Models containing bilayer desorption, dendrimer internalization in the bilayer, or dendrimer translocation did not properly simultaneously fit all contrasts in the experimental data, as visualized in Figure S3 of the Supporting Information. The approach of simultaneous fitting all contrasts to the same model was validated by measuring the reflectivity in D_2O before and after solvent exchange to H_2O and cmSi (Figure S6A of the Supporting Information). All parameters used in the NR models can be found in Table S1 of the Supporting Information.

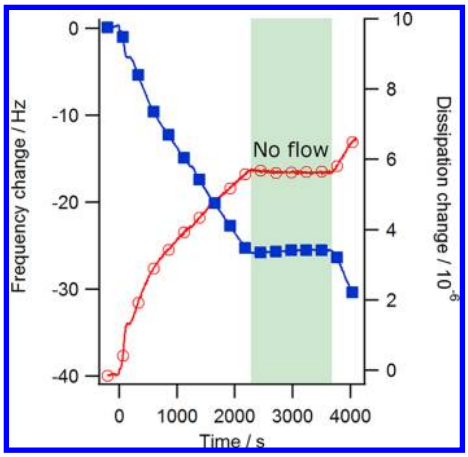

Figure 2. Effect of continuous flow on dendrimer adsorption to a POPC SLB as measured by QCM-D. PAMAM dendrimers (8 μM) were added at t = 0 s. No flow occurred between t = 2200 and 3700 s, which quickly leads to steady-state conditions. Further adsorption is observed upon resuming flow at 3700 s. For clarity, an offset is performed prior to dendrimer addition, only the 7th harmonics for the frequency (filled squares) and dissipation (open circles) are shown, and only 10% of the measured points are shown as markers.

POPG-Containing Bilayers. PAMAM G6 contains 256 positive surface charges at physiological pH.[31,32] Fluorescence microscopy showed that labeled dendrimers adsorbed to a greater extent to the surface of giant unilamellar vesicles (GUVs) composed of POPC/POPG, as compared to those formed by pure POPC,[17] mainly because of enhanced electrostatic interactions between the dendrimers and the SLB-containing POPG. The adsorption of dendrimers to the membrane eventually led, at a certain dendrimer concentration, to vesicle destabilization and collapse, inducing a multilamellar-like structure on the microscope slides. Figure 4 shows QCM-D experiments for the titration of PAMAM G6 dendrimer to SLBs formed by POPC and POPG at a 3:1 phosphocholine (PC)/phosphoglycerol (PG) molar ratio. In this case, dendrimers are flushed under continuous flow until t = 350 s (indicated by the arrow in Figure 4A). For low dendrimer concentrations, only adsorption occurred (red in Figure 4). However, the

dx.doi.org/10.1021/la3027144 | Langmuir 2012, 28, 13025−13033

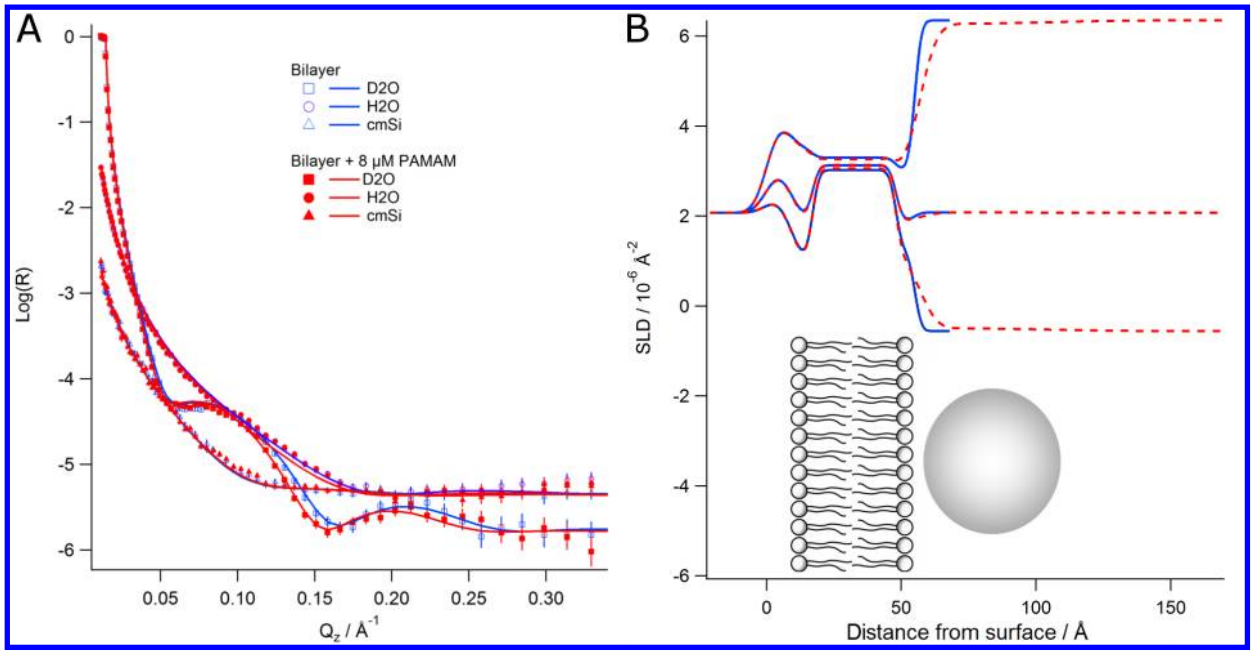

Figure 3. NR measurements of a POPC SLB before and after the addition of 8 μM PAMAM G6 dendrimer. (A) Reflectivity profiles for the measurements (symbol) and best corresponding fit (line). (B) SLD profiles for models used to fit experimental reflectivity profiles before (solid lines) and after (dashed lines) dendrimer addition. In this case, about 10 mL of dendrimer solution was flushed in the cell prior to performing the NR measurement. The inset in B shows schematics for the proposed model.

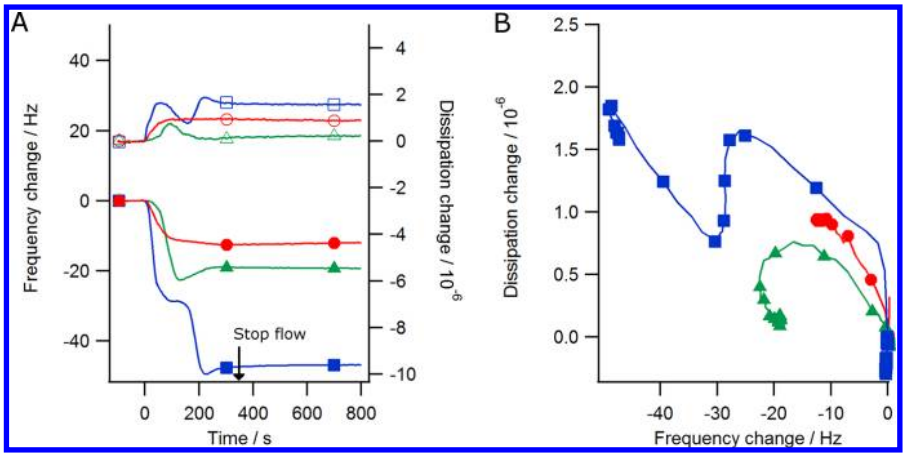

Figure 4. Addition of PAMAM dendrimers to a bilayer composed of POPC and POPG in a molar ratio of 3:1. Three dendrimer concentrations, 0.1 μM (circle, red), 1 μM (triangle, green), and 8 μM (square, blue), are added to the bilayers at t = 0 s in a continuous flow until t = 360 s when the flow is stopped. Markers are only shown for a portion of the data points to aid in the identification of the curves. (A) Change in frequency (filled symbols) and dissipation (open symbol) upon dendrimer addition. (B) Change in dissipation against change in frequency. For clarity, only the 7th harmonics are shown, an offset is performed prior to dendrimer addition, and only 10% of the measured points are shown as markers. For the same reasons, the bilayer formation is not shown. Typical frequency and dissipation changes upon formation of a SLB are shown in Figure S1 of the Supporting Information.

mechanism of interaction changed upon increasing the dendrimer concentration. For the higher concentrations (blue and green in Figure 4), the initial adsorption is followed by a decrease in both frequency and dissipation, indicating that desorption occurs. This is followed by a second adsorption step for the highest dendrimer concentration used (8 μM, blue in Figure 4). This complex mechanism of interaction is easier visualized in the F/D plot (Figure 4B), where several mechanistic steps can be observed as lines with different slopes. First, dendrimer adsorption induces a very steep line for which a small decrease in frequency was accompanied with a large increase in dissipation. Then, a less steeper slope is observed for the D/F plot, where the change in dissipation is also accompanied by a large change in frequency. Thus far, the F/D plots are similar to those observed for the titration of 8 μM dendrimers to a POPC SLB. However, when the frequency decrease reaches between −20 and −30 Hz, the dissipation suddenly decreases with no significant change in frequency. This signal indicates the formation of a stiffer adsorbed layer. For 8 μM dendrimers (blue in Figure 4), this is followed by a second increase in dissipation and a decrease of frequency, indicating that more wet mass is associated to the surface.

NR was performed on a POPC/POPG SLB, and the obtained reflectivity profiles and the best obtained fit, before and after the addition of 8 μM dendrimer, are shown in Figure S4 of the Supporting Information and Figure 5, respectively.

dx.doi.org/10.1021/la3027144 | *Langmuir* 2012, 28, 13025−13033

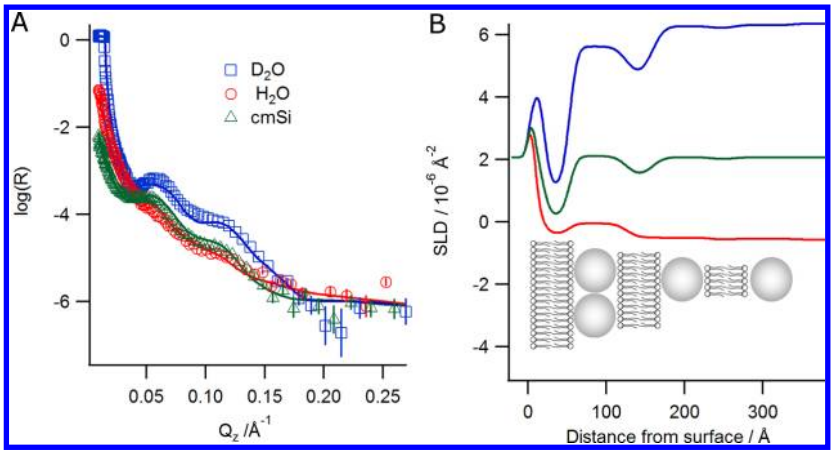

Figure 5. NR measurement of 8 μM PAMAM dendrimer added to a bilayer composed of POPC and POPG in a molar ratio of 3:1. (A) Reflectivity profiles and best obtained fit to the data for three contrasts. (B) SLD profile for the used model. Reflectivity profiles and best obtained fit to the bilayer prior to dendrimer addition is shown in Figure S4 of the Supporting Information.

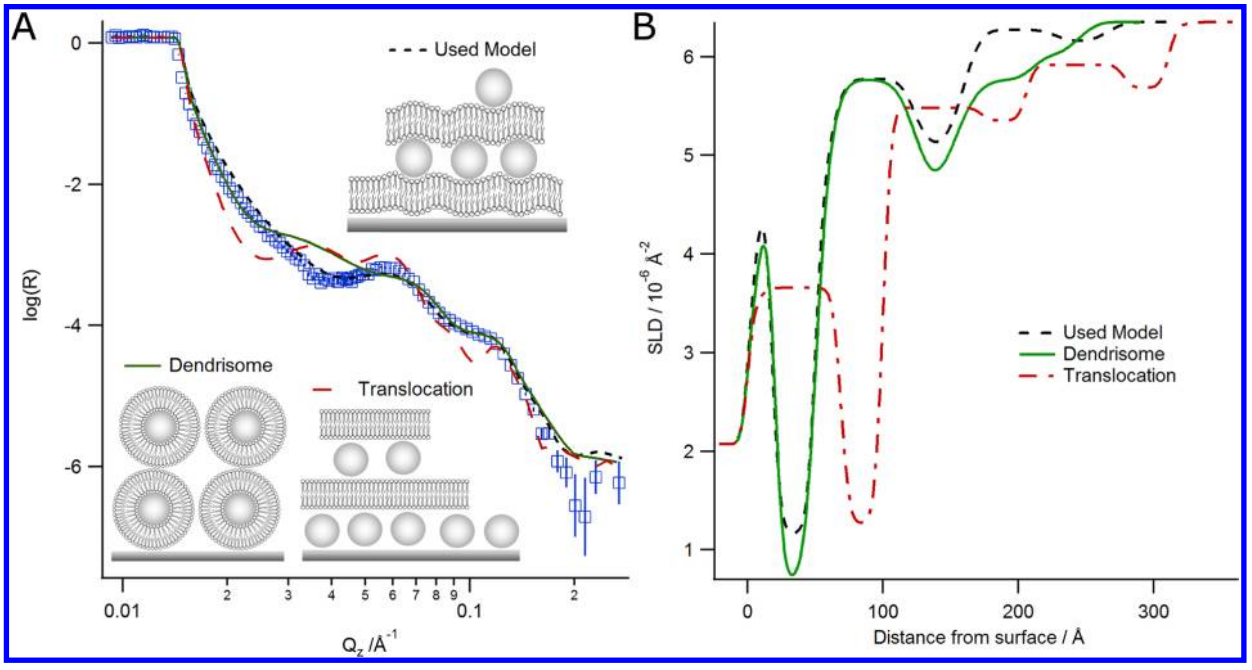

Figure 6. NR profile of 8 μM PAMAM G6 dendrimers added to a PG-containing SLB. Best obtained fit with dendrimer translocation (red dashed line), formation of dendrisomes (green solid line), and the model that we used (black dashed line). For clarity, only D_2O contrast is shown, although the isotropic contrast cmSi and H_2O were included to find the best fit for each model. Given that the spacing of the fringes corresponds to a lamellar phase, SLD for a layer of dendrisomes was calculated according to $SLD_{dendrisome} = (SLD_{G6}A_{G6} + SLD_{tail}A_{tail})/(A_{tail} + A_{G6})$, where A_{G6} and A_{tail} are cross-sectional areas of a dendrimer assuming a sphere with a radius of 35 Å and a 30 Å thick lipid layer surrounding the dendrimer, respectively, and SLD_{G6} and SLD_{tail} are the scattering length densities for dendrimers and lipid tails, respectively.

Because of a small difference in SLD between dendrimers (2.5×10^{-6} Å^2) and lipid tails of the mixed lipid bilayer, fully hydrogenated (-0.3×10^{-6} Å^2) instead of perdeuterated (3.2×10^{-6} Å^2) POPC lipids were used to achieve maximum contrast between the mixed lipid tails and the dendrimers. Note that, for the addition of dendrimer to POPG-containing SLB, the reflectivity profiles dramatically differ from those measured for POPC bilayers only. In the POPG case, the reflectivity shows several Kiessig fringes, indicating a major rearrangement in the SLB. The periodicity of the fringes indicates that the adsorbed film has a repeating distance of about 100 Å. This corresponds to the thickness of the lipid bilayer (50 Å) and the diameter of a dendrimer (50 Å; see data for dendrimer adsorption on SiO_2 in Figure S5 of the Supporting Information, in agreement with previous studies).[33] Note that dendrimer layer thickness is slightly thinner than the size of dendrimers measured in solution.[34] This apparent contradiction is in line with the results by Mecke et al.[35] and Kelly et al.,[36] where the dendrimers deformed and flattened at the surface of silicon and fluid lipid bilayers, respectively. Although the fringes are not as sharp as "real" Bragg peaks, the position of the maxima in the fringes (Q = 0.058 and 0.012 Å^{-1}) with the repetitions 1:1 and 2:1 indicate that a lamellar phase is formed. Such a structure could be obtained from dendrimers adsorbing on top of a lipid bilayer or for dendrimers that lifted up the lipid bilayer upon translocation. Another possibility is the formation of an adsorbed layer of lipid-coated dendrimers, so-called dendrisomes. Figure 6 clearly shows that neither the model for

dx.doi.org/10.1021/la3027144 | *Langmuir* 2012, 28, 13025−13033

translocation nor dendrisome formation can properly represent the experimental data. Instead, the model that best fits the data involves dendrimer adsorption on top of the lipid bilayer.

The model that best fits the reflectivity data (Figure 5) involves three lipid bilayer patches sandwiched in between dendrimer molecules, as schematically represented in the insertion of Figure 5A. Furthermore, in this model, the lipid headgroups and dendrimers are fused into a single layer with high interfacial roughness, as seen in Table S1 of the Supporting Information. The fact that dendrimers and lipid headgroups cannot be separated indicates that the dendrimers and lipid headgroups are interdigitated or that the dendrimers induce a certain degree of fluctuations in the lipid bilayer, as the bilayer changes its curvature to slightly bend around the dendrimers (see schematics in Figure 7). However, we cannot

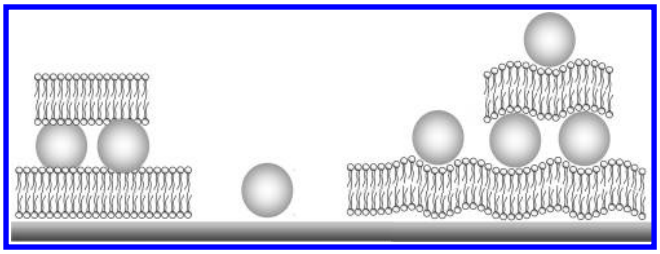

Figure 7. Schematics of dendrimer addition to a POPG-containing SLB according to the model giving the best fit to NR experimental data. Lipids are removed from the surface, and stacks of bilayer patches are bridged together by dendrimers. The inner bilayer could contain up to 4% dendrimers, which are then most likely located at empty spaces of the silica surface because of defects in the SLB. Lipid headgroups and dendrimers can be modeled as one layer, indicating that the dendrimers might be intercalated with the lipid headgroups (left) or that the dendrimers induce the formation of a large-scale roughness (right).

rule out that this effect is due to the small difference in SLD between the lipid headgroups (1.97×10^{-6} Å^2) and the dendrimers (2.5×10^{-6} Å^2). Because of the fitting uncertainty, our model could also allow up to 4% dendrimers co-adsorbed at the SiO_2 surface. These dendrimers, if any, are likely adsorbed to the silica surfaces in bilayer defects, as previously observed by atomic force microscopy (AFM) imaging.[11,37] Finally, although highly unlikely because of energetic considerations, we cannot exclude that these 4% dendrimers are inserted in the bilayer, as proposed by molecular dynamics (MD) simulations for dendrimers of generations five and seven.[38]

From the fits, it is clear that, even under strengthened electrostatic conditions, dendrimers are not able to fully translocate across the bilayer. At high dendrimer concentrations, dendrimers not only adsorbed to the SLB but also partially removed some lipids from the inner bilayer and built stacks. The dendrimers are localized in between the patches of lipid bilayer. The results indeed resemble the stacking observed after dendrimer interaction with GUVs containing POPC and POPG, as well as lamellar structures observed in the condensed gel phase.[17,34]

DISCUSSION

As expected, both NR and QCM-D experiments show that the highly cationic dendrimers are more prone to interact with bilayers carrying a net negative charge (POPG-containing membranes) than bilayers with a net zero charge (pure POPC membranes). Even for the zwitterionic POPC bilayers, NR experiments show that a small amount of dendrimers could adsorb to the membrane but models containing dendrimer translocation, lipid removal, or intercalation into the membrane could not be used to simultaneously fit all of the contrasts in the data (see Figure S4 of the Supporting Information). The QCM-D experiments also show that dendrimer adsorption on SLBs gives rise to an increase in dissipation. Adsorption of dendrimers on silica surfaces (see Figure S5 of the Supporting Information) causes almost no increase in dissipation, indicating that a more mobile dendrimer layer is created on the POPC bilayer, as compared to the silica surface. This could be due to stronger electrostatic interactions between the highly cationic dendrimers and the negatively charged silica surface, as compared to the zwitterionic lipid bilayer or the fluidity of the lipid bilayer that may allow the dendrimer to diffuse and roll along the bilayer surface. The less tightly bound dendrimers on the POPC bilayer might be free to move as the crystal oscillates, inducing the observed dissipation increase. Similar F/D signals were previously observed for individual objects adsorbed to QCM-D crystals.[27−29] It is important to note that, in the QCM-D, not only lipids and dendrimers contribute to the signal but also water coupled to the surface adds to the measured signal. For heterogeneous films, coupled water has shown to account for a significant part of the dissipation response.[29,39] This might be one of the reasons for the larger apparent effect of dendrimer addition to POPC SLBs as observed in the QCM-D experiments compared to the NR experiments. Another difference in the experimental setup for the experiments with POPC bilayers is the usage of a continuous flow in the QCM-D experiments, while after injection of about 10 mL of dendrimer solution, no flow was present in the NR experiment. Hence, the total cell volume is exchanged about 150 times within the complete QCM-D experiments, while it is only exchanged about 10 times in the NR experiment. Furthermore, the interfacial diffusion layer is considerably smaller for the QCM-D setup because the experiment is performed under constant flow, while there was neither constant flow nor stirring in the NR measurement. Figure 2 showed that the degree of change in dissipation and frequency upon dendrimer exposure to a POPC SLB largely depended upon how much solution was flown into the liquid cell. Differences in the flow rate and volume are likely to be the main cause for the increased adsorption observed for QCM-D experiments compared to NR experiments.

When POPG is present in the SLB, the electrostatic interaction with the dendrimers increases and, overall, a different interaction mechanism between the SLB and dendrimers is observed, as sensed by QCM-D. Our NR experiments show that dendrimers adsorb to the bilayer, bridging together patches of bilayers formed by removal of lipids from the inner bilayer. These results are in good agreement with the QCM-D experiments, where different slopes in the F/D plots are observed that include a shift to slower motions of the dendrimers on the SLB upon increased coverage, followed by stiffening of the film probably because of the loss of water upon rearrangement of the SLB, and finally further adsorption of dendrimers on the SLB. Similar results were reported earlier for GUVs containing POPG, where dendrimers bridged together and destabilized vesicles, eventually leading to their collapse and formation of stacks of bilayers and dendrimers. Dendrimers have also been found to bridge small unilamellar vesicles (SUVs), leading to increased

dx.doi.org/10.1021/la3027144 | *Langmuir* 2012, 28, 13025−13033

mixing of lipids.[40] The results are in good agreement with measurements on the condensed lamellar phase formed, where dendrimers bridge together bilayers.[34]

Figure 7 gives a schematic representation of possible explanations to the model used to fit the NR data upon the addition of dendrimers to a POPG-containing bilayer. This model could include up to 4% dendrimers coexisting with the bilayer closest to the surface, most likely located within defects of the SLB, as previously observed by imaging AFM.[11,37] Regardless of the eventual presence of dendrimers at the SiO_2 surface, models in which dendrimers translocate the SLB and form a dendrimer layer underneath the lipid bilayer could not be used to fit our data (see Figure 6). Previously, Ainalem et al.[41] suggested that dendrimers were indeed able to translocate across zwitterionic SLBs at low ionic conditions (10 mM NaBr), as measured by NR. The differences in ionic strength are not likely the cause for the reported differences in mechanism, because we also studied PG-containing bilayers, where stronger electrostatic forces are expected. However, there is a major difference in the experimental setup between our experiment and that performed by Ainalem et al.:[41] stirring was used in the latter case. Figure 2 clearly shows that dendrimer adsorption is enhanced upon continuous flow. Similar enhancement and a major structural effect on the interfacial layer are expected upon stirring.

Previously, removal of lipids by dendrimers was proposed to be induced via the formation of dendrisomes (dendrimers coated by lipid bilayers).[12,36,37] The energy required to bend the bilayer around the dendrimers in an unfavorable curvature is in this case gained by the favorable electrostatic interaction between the lipid heads and the terminal groups of the dendrimers. Because of a smaller number of terminal groups and a smaller radius, dendrimers of generation six or smaller are not capable of individually supporting a surrounding vesicle.[12,36] This is in agreement with our NR data, for which models containing dendrisomes could not be used to fit the data (see Figure 6). Similar results were found by SAXS measurements on the condensed gel phase formed by PAMAM G6 dendrimers and POPG-containing vesicles at relatively high concentrations.[34] These measurements established that, at a critical dendrimer/lipid molar ratio, a gel phase with a lamellar structure was formed. A gel phase of dendrisomes should give a hexagonal packing instead.

For the lower dendrimer generations, it is instead proposed that dendrimers are able to deform and flatten out on the bilayer to maximize the bilayer−dendrimer interaction.[11,36,41,42] MD simulations showed that PAMAM dendrimers of generation three flatten out on fluid l-α-dimyristoylphosphatidylcholine (DMPC) bilayers,[42] also corroborated by AFM images.[11] AFM has also been used to show that dendrimers deform upon binding to the negatively charged mica surfaces.[35] To fit our experimental NR data for dendrimers added to bilayer-containing POPG, we used a model in which the lipid headgroups and dendrimers are modeled as a single layer with high interfacial roughness. This suggests that the dendrimers might be intercalated in the bilayer headgroup region or that a large-scale roughness is generated as the bilayer changes curvature to follow the shape of the dendrimers, as shown in Figure 7 (left and right schematics, respectively). Several other techniques support the ability of dendrimers to change the membrane curvature.[40,41,43] There is, however, the possibility that the low difference in SLD between the lipid headgroups (1.97×10^{-6} Å^2) and the dendrimers (2.4×10^{-6} Å^2) does not allow for distinguishing the molecules as separated layers, although that was not the case for pure POPC SLBs.

For the final application of dendrimers as drug delivery vehicles, their capability to enter into the target cell must be secured. Several cell studies indicate that dendrimers are indeed taken up by the cell via clathrin or caveol pathways.[7−10] Passive translocation, on the other hand, has been argued on the basis of the ability of dendrimers to create large holes in SLB,[7] although our recent fluorescence microcopy studies did not support passive translocation across GUVs.[17] Our NR measurements showed that dendrimers (PAMAM G6) do not to any significant extent passively translocate across model membranes in the experimental conditions used, regardless of the membrane surface charge. Therefore, it is likely that PAMAM G6 dendrimers can only enter into cells via protein-mediated endocytosis pathways, as previously suggested in cell studies.[44−46] Finally, the higher activity of PAMAM dendrimers toward POPG-containing membranes, as compared to pure PC membranes, is in line with the earlier demonstrated antibacterial activity of PAMAM dendrimers against Gram-negative bacteria at concentrations in which PAMAM dendrimers were not cytotoxic against human epithelial cells.[47]

■ CONCLUSION

Using QCM-D and NR measurements, it was possible to characterize PAMAM G6 dendrimer interaction with model membranes composed of mixtures of POPG and POPC, at physiological relevant conditions in terms of ionic strength and pH. Previous experiments performed in our group using GUVs determined that dendrimers cannot passively translocate the membrane to be released into the vesicle lumen. However, these experiments could not elucidate whether dendrimers were able to translocate but stay attached to the membrane. Using NR and QCM-D measurements, we have now shown that dendrimers adsorb to bilayers without effectively translocating the membrane. Upon enhanced electrostatic conditions, dendrimers are able to structurally rearrange the SLB, creating stacks of bilayer−dendrimer sheets and thereby maximizing the dendrimer−lipid interaction. This indicates that dendrimers need to actively be transported through cell membranes by protein-mediated endocytosis, in agreement with previous cell studies.[44−46]

■ ASSOCIATED CONTENT

Ⓢ Supporting Information

QCM-D signal for typical bilayer formation (Figure S1), QCM-D signal upon dendrimer adsorption to POPC SLB for all of the measured harmonics (Figure S2), all NR models for dendrimer adsorption to POPC SLB (Figure S3), NR profiles for POPC/POPG SLB (Figure S4), QCM-D and NR measurements for dendrimer adsorption on SiO_2 surfaces (Figure S5), NR profiles before and after rinsing the system with PBS buffer (Figure S6), and table with all parameters used in NR models (Table S1). This material is available free of charge via the Internet at http://pubs.acs.org.

■ AUTHOR INFORMATION

Corresponding Author

*E-mail: cardenas@nano.ku.dk.

Author Contributions

The manuscript was written through contributions of all authors. All authors have given approval to the final version of the manuscript.

Funding

The authors gratefully acknowledge financial support from the "Center for Synthetic Biology" at Copenhagen University funded by the UNIK research initiative of the Danish Ministry of Science, Technology and Innovation and DANSCATT center funded by the Danish government.

Notes

The authors declare no competing financial interest.

■ ACKNOWLEDGMENTS

We thank the neutron scattering facilities Institut Laue Langevin (France) and ISIS at the Rutherford Appleton Laboratory (U.K.) for allocated beam time. In particular, we thank Max Skoda (ISIS) for further local support.

■ ABBREVIATIONS USED

d_{31}-POPC, 1-palmoyl(d_{31})-2-oleoyl-*sn*-glycero-3-phosphocholine; GUV, giant unilamellar vesicle; PAMAM, poly(aminoamide); POPC, 1-palmitoyl-2-oleoyl-*sn*-glycero-3-phosphocholine; POPG, 1-palmitoyl-2-oleoyl-*sn*-glycero-3-phospho(1′-*rac*-glycerol); SLB, supported lipid bilayer; SLD, scattering length density; QCM-D, quartz crystal microbalance with dissipation monitoring

■ REFERENCES

(1) Asthana, A.; Chauhan, A. S.; Diwan, P. V.; Jain, N. K. Poly(amidoamine) (PAMAM) dendritic nanostructures for controlled site-specific delivery of acidic anti-inflammatory active ingredient. *AAPS PharmSciTech* **2005**, *6* (3), E536−E542.

(2) Choi, S. K.; Thomas, T.; Li, M. H.; Kotlyar, A.; Desai, A.; Baker, J. R. Light-controlled release of caged doxorubicin from folate receptor-targeting PAMAM dendrimer nanoconjugate. *Chem. Commun.* **2010**, *46* (15), 2632−2634.

(3) Dong, Z. Q.; Hamid, K. A.; Gao, Y.; Lin, Y. L.; Katsumi, H.; Sakane, T.; Yamamoto, A. Polyamidoamine dendrimers can improve the pulmonary absorption of insulin and calcitonin in rats. *J. Pharm. Sci.* **2011**, *100* (5), 1866−1878.

(4) Huang, J.; Gao, F.; Tang, X. X.; Yu, J. H.; Wang, D. X.; Liu, S. Y.; Li, Y. P. Liver-targeting doxorubicin-conjugated polymeric prodrug with pH-triggered drug release profile. *Polym. Int.* **2010**, *59* (10), 1390−1396.

(5) Kobayashi, H.; Sato, N.; Kawamoto, S.; Saga, T.; Hiraga, A.; Ishimori, T.; Konishi, J.; Togashi, K.; Brechbiel, M. W. Novel intravascular macromolecular MRI contrast agent with generation-4 polyamidoamine dendrimer core: Accelerated renal excretion with coinjection of lysine. *Magn. Reson. Med.* **2001**, *46* (3), 457−464.

(6) Tomalia, D. A.; Baker, H.; Dewald, J.; Hall, M.; Kallos, G.; Martin, S.; Roeck, J.; Ryder, J.; Smith, P. A new class of polymers—Starburst-dendritic macromolecules. *Polym. J.* **1985**, *17* (1), 117−132.

(7) Parimi, S.; Barnes, T. J.; Callen, D. F.; Prestidge, C. A. Mechanistic insight into cell growth, internalization, and cytotoxicity of PAMAM dendrimers. *Biomacromolecules* **2010**, *11* (2), 382−389.

(8) Kitchens, K. M.; Foraker, A. B.; Kolhatkar, R. B.; Swaan, P. W.; Ghandehari, H. Endocytosis and interaction of poly(amidoamine) dendrimers with Caco-2 cells. *Pharm. Res.* **2007**, *24* (11), 2138−2145.

(9) Saovapakhiran, A.; D'Emanuele, A.; Attwood, D.; Penny, J. Surface modification of PAMAM dendrimers modulates the mechanism of cellular internalization. *Bioconjugate Chem.* **2009**, *20* (4), 693−701.

(10) Albertazzi, L.; Storti, B.; Marchetti, L.; Beltram, F. Delivery and subcellular targeting of dendrimer-based fluorescent pH sensors in living cells. *J. Am. Chem. Soc.* **2010**, *132* (51), 18158−18167.

(11) Erickson, B.; DiMaggio, S. C.; Mullen, D. G.; Kelly, C. V.; Leroueil, P. R.; Berry, S. A.; Baker, J. R.; Orr, B. G.; Holl, M. M. B. Interactions of poly(amidoamine) dendrimers with Survanta lung surfactant: The importance of lipid domains. *Langmuir* **2008**, *24* (19), 11003−11008.

(12) Mecke, A.; Majoros, I. J.; Patri, A. K.; Baker, J. R.; Holl, M. M. B.; Orr, B. G. Lipid bilayer disruption by polycationic polymers: The roles of size and chemical functional group. *Langmuir* **2005**, *21* (23), 10348−10354.

(13) Leroueil, P. R.; Berry, S. A.; Duthie, K.; Han, G.; Rotello, V. M.; McNerny, D. Q.; Baker, J. R.; Orr, B. G.; Holl, M. M. B. Wide varieties of cationic nanoparticles induce defects in supported lipid bilayers. *Nano Lett.* **2008**, *8* (2), 420−424.

(14) Hong, S. P.; Bielinska, A. U.; Mecke, A.; Keszler, B.; Beals, J. L.; Shi, X. Y.; Balogh, L.; Orr, B. G.; Baker, J. R.; Holl, M. M. B. Interaction of poly(amidoamine) dendrimers with supported lipid bilayers and cells: Hole formation and the relation to transport. *Bioconjugate Chem.* **2004**, *15* (4), 774−782.

(15) Lee, H.; Larson, R. G. Molecular dynamics simulations of PAMAM dendrimer-induced pore formation in DPPC bilayers with a coarse-grained model. *J. Phys. Chem. B* **2006**, *110* (37), 18204−18211.

(16) Shcharbin, D.; Drapeza, A.; Loban, V.; Lisichenok, A.; Bryszewska, M. The breakdown of bilayer lipid membranes by dendrimers. *Cell. Mol. Biol. Lett.* **2006**, *11* (2), 242−248.

(17) Åkesson, A.; Veje Lundgaard, C.; Ehrlich, N.; Günter Pomorski, T.; Stamou, D.; Cárdenas, M. Induced dye leakage by PAMAM G6 does not imply dendrimer entry into vesicle lumen. *Soft Matter* **2012**, *8*, 8972−8980.

(18) Koenig, B. W.; Gawrisch, K.; Krueger, S.; Orts, W.; Majkrzak, C. F.; Berk, N.; Silverton, J. V. Membrane structure at the solid/water interface studied with neutron reflectivity and atomic force microscopy. *Biophys. J.* **1996**, *70* (2), Wp229−Wp229.

(19) Hayter, J. B.; Highfield, R. R.; Pullman, B. J.; Thomas, R. K.; McMullen, A. I.; Penfold, J. Critical reflection of neutrons—A new technique for investigating interfacial phenomena. *J. Chem. Soc., Faraday Trans. 1* **1981**, *77*, 1437−1448.

(20) Penfold, J.; Richardson, R. M.; Zarbakhsh, A.; Webster, J. R. P.; Bucknall, D. G.; Rennie, A. R.; Jones, R. A. L.; Cosgrove, T.; Thomas, R. K.; Higgins, J. S.; Fletcher, P. D. I.; Dickinson, E.; Roser, S. J.; McLure, I. A.; Hillman, A. R.; Richards, R. W.; Staples, E. J.; Burgess, A. N.; Simister, E. A.; White, J. W. Recent advances in the study of chemical surfaces and interfaces by specular neutron reflection. *J. Chem. Soc., Faraday Trans.* **1997**, *93* (22), 3899−3917.

(21) Cubitt, R.; Fragneto, G. D17: The new reflectometer at ILL. *Appl. Phys. A: Mater. Sci. Process.* **2002**, *74*, S329−S331.

(22) Nelson, A. Co-refinement of multiple-contrast neutron/X-ray reflectivity data using MOTOFIT. *J. Appl. Crystallogr.* **2006**, *39*, 273−276.

(23) Armen, R. S.; Uitto, O. D.; Feller, S. E. Phospholipid component volumes: Determination and application to bilayer structure calculations. *Biophys. J.* **1998**, *75* (2), 734−744.

(24) Kucerka, N.; Holland, B. W.; Gray, C. G.; Tomberli, B.; Katsaras, J. Scattering density profile model of POPG bilayers as determined by molecular dynamics simulations and small-angle neutron and X-ray scattering experiments. *J. Phys. Chem. B* **2012**, *116* (1), 232−239.

(25) van Meer, G.; Voelker, D. R.; Feigenson, G. W. Membrane lipids: Where they are and how they behave. *Nat. Rev. Mol. Cell Biol.* **2008**, *9* (2), 112−124.

(26) Epand, R. M.; Epand, R. F. Domains in bacterial membranes and the action of antimicrobial agents. *Mol. BioSyst.* **2009**, *5* (6), 580−587.

(27) Johannsmann, D.; Reviakine, I.; Rojas, E.; Gallego, M. Effect of sample heterogeneity on the interpretation of QCM(-D) data: Comparison of combined quartz crystal microbalance/atomic force

microscopy measurements with finite element method modeling. *Anal. Chem.* **2008**, *80* (23), 8891−8899.
(28) Johannsmann, D.; Reviakine, I.; Richter, R. P. Dissipation in films of adsorbed nanospheres studied by quartz crystal microbalance (QCM). *Anal. Chem.* **2009**, *81* (19), 8167−8176.
(29) Reviakine, I.; Johannsmann, D.; Richter, R. P. Hearing what you cannot see and visualizing what you hear: Interpreting quartz crystal microbalance data from solvated interfaces. *Anal. Chem.* **2011**, *83* (23), 8838−8848.
(30) Åkesson, A.; Lind, T.; Ehrlich, N.; Stamou, D.; Wacklin, H.; Cárdenas, M. Composition and structure of mixed phospholipid supported bilayers formed by POPC and DPPC. *Soft Matter* **2012**, *8* (20), 5658−5665.
(31) Esfand, R.; Tomalia, D. A. Poly(amidoamine) (PAMAM) dendrimers: From biomimicry to drug delivery and biomedical applications. *Drug Discovery Today* **2001**, *6* (8), 427−436.
(32) Cakara, D.; Kleimann, J.; Borkovec, M. Microscopic protonation equilibria of poly(amidoamine) dendrimers from macroscopic titrations. *Macromolecules* **2003**, *36* (11), 4201−4207.
(33) Ainalem, M. L.; Campbell, R. A.; Nylander, T. Interactions between DNA and poly(amido amine) dendrimers on silica surfaces. *Langmuir* **2010**, *26* (11), 8625−8635.
(34) Akesson, A.; Bendtsen, K. M.; Beherens, M. A.; Pedersen, J. S.; Alfredsson, V.; Gomez, M. C. The effect of PAMAM G6 dendrimers on the structure of lipid vesicles. *Phys. Chem. Chem. Phys.* **2010**, *12* (38), 12267−12272.
(35) Mecke, A.; Lee, I.; Baker, J. R.; Holl, M. M. B.; Orr, B. G. Deformability of poly(amidoamine) dendrimers. *Eur. Phys. J. E: Soft Matter Biol. Phys.* **2004**, *14* (1), 7−16.
(36) Kelly, C. V.; Liroff, M. G.; Triplett, L. D.; Leroueil, P. R.; Mullen, D. G.; Wallace, J. M.; Meshinchi, S.; Baker, J. R.; Orr, B. G.; Holl, M. M. B. Stoichiometry and structure of poly(amidoamine) dendrimer−lipid complexes. *ACS Nano* **2009**, *3* (7), 1886−1896.
(37) Mecke, A.; Uppuluri, S.; Sassanella, T. M.; Lee, D. K.; Ramamoorthy, A.; Baker, J. R.; Orr, B. G.; Holl, M. M. B. Direct observation of lipid bilayer disruption by poly(amidoamine) dendrimers. *Chem. Phys. Lipids* **2004**, *132* (1), 3−14.
(38) Lee, H.; Larson, R. G. Coarse-grained molecular dynamics studies of the concentration and size dependence of fifth- and seventh-generation PAMAM dendrimers on pore formation in DMPC bilayer. *J. Phys. Chem. B* **2008**, *112* (26), 7778−7784.
(39) Tellechea, E.; Johannsmann, D.; Steinmetz, N. F.; Richter, R. P.; Reviakine, I. Model-independent analysis of QCM data on colloidal particle adsorption. *Langmuir* **2009**, *25* (9), 5177−5184.
(40) Zhang, Z. Y.; Smith, B. D. High-generation polycationic dendrimers are unusually effective at disrupting anionic vesicles: Membrane bending model. *Bioconjugate Chem.* **2000**, *11* (6), 805−814.
(41) Ainalem, M. L.; Campbell, R. A.; Khalid, S.; Gillams, R. J.; Rennie, A. R.; Nylander, T. On the ability of PAMAM dendrimers and dendrimer/DNA aggregates to penetrate POPC model biomembranes. *J. Phys. Chem. B* **2010**, *114* (21), 7229−7244.
(42) Kelly, C. V.; Leroueil, P. R.; Orr, B. G.; Holl, M. M. B.; Andricioaei, I. Poly(amidoamine) dendrimers on lipid bilayers II: Effects of bilayer phase and dendrimer termination. *J. Phys. Chem. B* **2008**, *112* (31), 9346−9353.
(43) Lee, H.; Larson, R. G. Lipid bilayer curvature and pore formation induced by charged linear polymers and dendrimers: The effect of molecular shape. *J. Phys. Chem. B* **2008**, *112* (39), 12279−12285.
(44) Albertazzi, L.; Serresi, M.; Albanese, A.; Beltram, F. Dendrimer internalization and intracellular trafficking in living cells. *Mol. Pharmaceutics* **2010**, *7* (3), 680−688.
(45) Perumal, O. P.; Inapagolla, R.; Kannan, S.; Kannan, R. M. The effect of surface functionality on cellular trafficking of dendrimers. *Biomaterials* **2008**, *29* (24−25), 3469−3476.
(46) Jevprasesphant, R.; Penny, J.; Attwood, D.; McKeown, N. B.; D'Emanuele, A. Engineering of dendrimer surfaces to enhance transepithelial transport and reduce cytotoxicity. *Pharm. Res.* **2003**, *20* (10), 1543−1550.
(47) Calabretta, M. K.; Kumar, A.; McDermott, A. M.; Cai, C. Z. Antibacterial activities of poly(amidoamine) dendrimers terminated with amino and poly(ethylene glycol) groups. *Biomacromolecules* **2007**, *8* (6), 1807−1811.